Analyst

PAPER

View Article Online
View Journal

Cite this: DOI: 10.1039/d5an01352f

Feasibility study of superoxide chemical ionization mass spectrometry (O_2^- CIMS) for real-time gas-phase measurements of per- and polyfluoroalkyl substances (PFAS)

Yufan Hu, †[a] Joji W. Sherman, †[b] Michael J. Davern,[a] Zane A. Alsebai,[a] Yoonsub Kim, [b] Yue Zhang,[c] Chenyang Bi, [d] Barbara J. Turpin [b] and Jason D. Surratt *[a,b]

Per- and polyfluoroalkyl substances (PFAS) are highly persistent pollutants with known adverse impacts on environmental and public health. Traditional gas-phase PFAS detection approaches often involve labor-intensive sample collection and preparation, while offering low temporal resolution. Alternatively, chemical ionization mass spectrometry (CIMS) allows for real-time airborne PFAS detection at sub-pptv sensitivity. While reagent ion generation often requires hazardous chemicals (*e.g.*, nitric acid, methyl iodide (I^-), and acetic anhydride), superoxide (O_2^-) CIMS provides a safer alternative and is better suited for mobile platforms where ventilation, space, and weight are constrained. O_2^- CIMS has five main reagent ions (*i.e.*, O_2^-, $(H_2O)O_2^-$, CO_3^-, $(CO_2)O_2^-$, and $CO_2(H_2O)O_2^-$) and low-background mass spectra above *m*/*z* 200. Thus, it is well suited to the relatively high molecular weights of airborne PFAS. Mass calibration was performed with a 5 : 1 fluorotelomer alcohol (FTOH) permeation tube. Ionization was found to occur mainly through deprotonation or adduct formation. Calibrations for fourteen environmentally- and industrially-relevant PFAS compounds are presented, including FTOHs, fluorotelomer diols, fluorinated sulfonamides, epoxides, and glycol ethers. While perfluoroalkyl carboxylic acids (PFCAs) were not detected, O_2^- CIMS offered higher sensitivity and lower detection/quantification limits than I^- CIMS for FTOHs; however, it remains a complementary PFAS measurement technique to I^- CIMS. Moreover, it yielded distinct fingerprint signals for FTOHs, confirming compound identification. This study demonstrates the utility of O_2^- CIMS for real-time airborne PFAS analysis in commonly encountered environments by capturing 6 : 2 FTOH gaseous emissions from fast-food packaging at room temperature, underscoring its strong promise for future development and applications.

Received 23rd December 2025,
Accepted 4th May 2026

DOI: 10.1039/d5an01352f

rsc.li/analyst

Introduction

Per- and polyfluoroalkyl substances (PFAS) are a class of synthetic chemicals that have been widely used in industry and consumer products since the mid-20th century.[1] Their strong carbon–fluorine bonds give them unique water- and grease-resistant properties, making them highly valued for their durability and versatility.[2–4] As a result, PFAS have been incorporated into a broad range of products, from everyday items to high-tech applications, including non-stick cookware, food packaging, water-repellent clothing, plumbing tape, refrigerants, firefighting foams, firefighter turnout gear, and semiconductor manufacturing.[3,5–14] However, while these chemicals offer significant functional benefits, they are highly mobile and persistent in the environment.[3,15] PFAS do not readily break down or biodegrade, leading to their accumulation in both living organisms and the environment over time.[16–18] This persistence has earned them the nickname "forever chemicals". Their widespread use and resistance to degradation have resulted in global contamination of air, soil, and water,[19] raising serious concerns about their environmental and ecological impacts, including potential disruption of ecosystems and entry into the food chain.[7,20,21] Studies have linked PFAS exposure to adverse human health effects, includ-

[a]Department of Chemistry, College of Arts and Sciences, University of North Carolina at Chapel Hill, Chapel Hill, North Carolina, USA 27514. E-mail: surratt@unc.edu; Tel: +919-966-0470; Fax: +919-966-7911
[b]Department of Environmental Sciences and Engineering, Gillings School of Global Public Health, University of North Carolina at Chapel Hill, Chapel Hill, North Carolina, USA 27599
[c]Department of Atmospheric Science, College of Arts and Sciences, Texas A&M University, College Station, Texas, USA 77843
[d]Aerodyne Research Inc., Billerica, Massachusetts, 01821, USA
† Both authors contributed equally to the work and are noted as co-first authors.

ing suppressed immune response, detrimental lipid profiles, neurobehavioral defects, and certain cancers.[22–25] Numerous research efforts are underway to address PFAS contamination through remediation strategies, including capture technologies and degradation methods.[26–31]

Current PFAS detection efforts are primarily focused on water and soil, not only because analytical techniques are relatively well-established, but also due to recent regulatory policies targeting water contamination,[28,32–37] as well as air measurements of PFAS being challenging.[38,39] However, investigating airborne PFAS is also important, as it helps explain the potential for atmospheric transport of PFAS to remote regions on Earth (*e.g.*, Arctic),[40,41] sheds light on their partitioning behavior in multiphase environments, and ultimately helps to resolve the sources of PFAS contamination in downwind private well water.[42–47] PFAS in air presents unique challenges, particularly in effectively collecting and storing these dilute and often volatile samples.[48] Traditional methods rely on sorbent materials or filters to collect samples over periods ranging from several hours to weeks, allowing PFAS concentrations to accumulate above instrumental detection limits.[48–50] After collection, samples are typically spiked with internal standards to correct for extraction recovery. Extracted samples are then concentrated and reconstituted for analysis by gas chromatography (GC) or liquid chromatography (LC) coupled with mass spectrometry (MS).[48,50–52] Though GC-/LC-MS provides two dimensions of compound confirmation (*i.e.*, retention time and mass), these offline methods require the use of expensive mass-labelled internal standards of PFAS.[48,50–52] While integrated samples have some advantages, their limitations also include significant time involved in sample processing and associated uncertainties. Moreover, the method only yields time-averaged PFAS concentrations over the sampling period with limited temporal resolution.

Chemical ionization mass spectrometry (CIMS) enables real-time gas-phase PFAS analysis using a soft ionization method.[53] Originally developed in the 1960s and 1970s, CIMS has significantly advanced in recent years.[54] Coupling chemical ionization (CI) with a time-of-flight (TOF) mass analyzer now allows for high-resolution MS detection and precise identification of complex compounds. Modern CIMS designs offer high sensitivity, enabling detection limits in the sub-pptv range, and are often compact and field-deployable, suitable for use on aircraft and mobile laboratories.[55,56] To best capture a wide array of compounds, CIMS employs different reagent ions that select for particular chemical properties, such as certain levels of volatility and oxidation states of carbon.[54,56] Reagent ions used in proton transfer reaction (PTR) systems, like H_3O^+ and NO^+, are standard for real-time monitoring of volatile organic compounds (VOCs).[57,58] Now it also has been used for volatile PFAS measurements.[59] Other reagent ions, such as I^- and NO_3^-, are commonly used for detecting oxygenated organics and highly oxidized organic gases.[54–56,60]

Iodide CIMS has previously been calibrated and applied to quantify oxygenated PFAS in the gas phase, including PFCAs from aqueous film-forming foam combustion,[61] and capturing 6 : 2 fluorotelomer alcohol (FTOH) emissions from rain jackets, floor wax applications, and microwaving popcorn.[62–65] However, there are notable limitations on using I^- CIMS. First of all, PFAS has a wide range of structures, but I^- is selective,[54,66] so it does not work for all species. Moreover, when the high molecular weight of PFAS adducts with I^-, which is a large ion, the high adduct weight makes it hard to be revolved in a TOFMS. Lastly, the reagent ions are generated by introducing pure nitrogen gas through a methyl iodide permeation tube,[62,67,68] which requires a robust ventilation system and secure exhaust handling for safe operation. These requirements limit their suitability for mobile laboratories, where space, weight, and ventilation capacity are constrained. Therefore, a safer alternative reagent ion that allows for detection of PFAS classes not previously detected by other CIMS methods and does not require the use of toxic chemicals (*e.g.*, methyl iodide) is needed. Superoxide (O_2^-), which can be generated more safely, has previously been used in detecting nitrates, sulfates, and highly oxygenated organic compounds, showing a non-selective but general reagent chemistry property.[69,70] Based on these results, superoxide may also show strong potential for real-time PFAS measurements in air. As a result, in this study we systematically examine the potential for O_2^- CIMS to make real-time quantitative measurements of airborne PFAS.

Materials and methods

Section S1 of SI provides suggested safety precautions when working with PFAS.

O_2^- ionization

For the setup (Fig. 1), considering previous methods,[70–72] compressed house air first passes through a Drierite Gas Purifier with 5A molecular sieves (Drierite 27068 L68GP Gas Purifier) to reduce humidity and remove impurities like CO_2, followed by a high-efficiency particulate air (HEPA) filter to remove particles. The cleaned air then flows through a NRD P-2021 Polonium-210 (Po-210) source at 2 liters per minute (LPM) to generate superoxide (O_2^-). These reagent ions are then transferred into the ion–molecule reactor (IMR), where they mix with gas-phase ambient samples at 80 mbar. Within the IMR, two dominant pathways are responsible for analyte ionization: deprotonation of the analyte (Reaction (R1)) and adduct formation with the reagent ion (Reaction (R2)). In some cases, analytes undergo additional adduct formation with water (H_2O) or carbon dioxide (CO_2), or they may fragment. Further details are provided in the Results and Discussion Section.

$$HX + O_2^- \rightarrow X^- + HO_2 \quad (R1)$$

$$HX + O_2^- \rightarrow HX(O_2)^- \quad (R2)$$

The resulting charged molecules pass through three differential vacuum chambers before entering the time-of-flight (TOF) mass analyzer for detection.[55] This allows for accurate

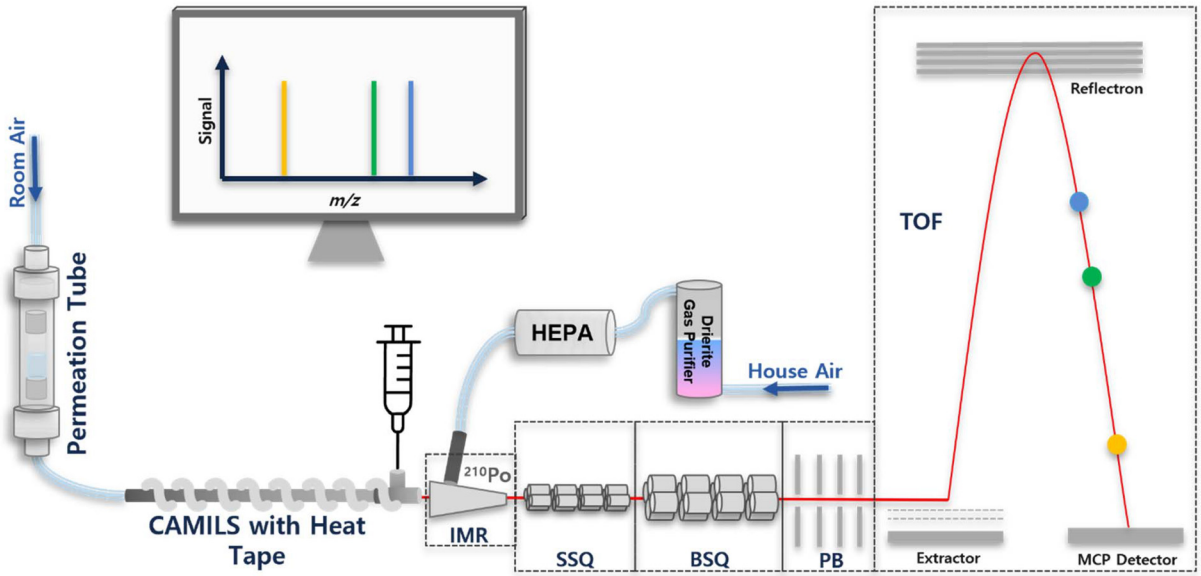

Fig. 1 O_2^- CIMS schematic diagram with CAMILS interfaced to inlet for PFAS calibrations. Reagent ions are generated using purified house air, and sampling flow uses room air, both at a flow rate of 2 LPM.

mass fittings and subsequent identification of molecular formulae.

PFAS calibrations

PFAS compounds for O_2^- CIMS calibration were selected based on their reported atmospheric and occupational relevances.[73] Section S2 describes standard information and preparation protocol. To aid the introduction of PFAS standards into the O_2^- CIMS, the Calibration Apparatus for Manual Injection of Liquid Standards (CAMILS),[62] a Restek sulfinert-coated Swagelok tee with GC septa used for liquid standard introduction for gas-phase PFAS analysis, was attached to the IMR as described previously by Davern *et al.*[62]

For each PFAS standard, 5, 10, 15, and 20 μL aliquots of 100 ng mL^{-1} and 1000 ng mL^{-1} solutions prepared in LC/MS grade methanol were injected in triplicate with a 25 μL Hamilton gastight syringe. More solvent selection information is discussed in the Results and Discussion Section (Fig. 3). Sufficient time was allotted between injections so that signals could return to the baseline. In some cases, to decrease this time, the temperature of the CAMILS increased up to 80 °C to encourage faster volatilization of the liquid standard. Each calibration was preceded by three 20 μL injections of methanol blanks to establish a background count for determining the sensitivity of calibrant ion peak *m*/*z* values. Limits of detection (LOD) and limits of quantitation (LOQ) were calculated as outlined in Bertram *et al.*, using a signal-to-noise ratio of 3 and 10, respectively.[55]

Permeation tube for mass calibration

Given the lack of abundant signals above *m*/*z* 200, there arose a need to introduce small but consistent reference ions for mass calibration. Based on the lab inventory, compound volatility, high molecular weight (MW), and detectable structural analogs, we selected 5 : 1 FTOH (MW 300 g mol^{-1}, and primarily detected by O_2^- CIMS as a superoxide adduct at *m*/*z* 332) to prepare a permeation tube for mass calibration. As it is less commonly reported than the more abundant *n* : 2 FTOHs (where n is an even number from 2 to 12), this compound is a suitable artificial standard, designed to minimize overlap with commonly occurring species found in ambient air.[51,64,65,73,74] The 5 : 1 FTOH permeation tube is made by using a permeation tube kit (Owlstone Inc.), and 99.0% pure 5 : 1 FTOH (Flouryx Labs). As this is not for quantification purposes, the emission rate was not characterized. At room temperature (20 °C), with a room air flow rate of 2 LPM, it provides a stable, trace level of 5 : 1 FTOH, which forms different adduct clusters with the reagent ions (*e.g.*, *M* + 32 and *M* + 94) allowing for its low-level continuous detection for mass calibration with little time required for equilibration. The O_2^- CIMS mass spectrum of 5 : 1 FTOH is provided in Section S3. The two 5 : 1 FTOH cluster peaks (*i.e.*, *m*/*z* 332 and 394) alongside other known reagent ion peaks (*i.e.*, *m*/*z* 32, 50, 60, 76 and 94, where details are provided in the Results and Discussion Section) were used as mass calibrants. The setup of the instrumentation is shown in Fig. 1, where the 5 : 1 FTOH permeation tube is placed upstream of the CAMILS to eliminate the contamination from standard injection in CAMILS. The impact of the permeation tube on reagent ion consumption is discussed in Section S4.

CIMS data collection and analysis

Data were collected using a high-resolution time-of-flight chemical ionization mass spectrometer (ToF-CIMS, Aerodyne Research Inc./TOFWERK AG), referred to as CIMS. It was characterized and described previously.[55,62,67,75] Tofware

Version 4.0.3 (Tofwerk AG) was used to analyze data. Instrument voltages, temperatures, and pressures were tuned to optimize sensitivity for I^- mode, which has been more well studied and characterized for PFAS air measurements. This was to prepare this method for CIMS operation with both I^- and O_2^- CIMS with rapid switching,[71] get it ready for future field deployment, and enable cross-comparison of sensitivities. Mass spectra were collected with a range of 11–824 Da, at 1 Hz frequency and an extraction period of 50 000 ns. More detailed instrument parameters including temperature, pressure and voltages can be found in Section S5.

Fast food package collection and storage

The fast-food paper wrap was obtained from a fast-food chain restaurant in Chapel Hill, NC, USA, and stored at room temperature and opened to ambient for a day before the analysis. After the perturbation experiment, the paper wrap was stored in a clear sandwich bag at room temperature. Half of it was then used for the GC-MS qualification.

Results and discussion

O_2^- CIMS mass spectrum, reagent ions, and normalization

Previously, O_2^- CIMS has been used to measure small molecules including methyl peroxide, hydrogen peroxide (H_2O_2),[72] ozone (O_3), and nitrogen dioxide (NO_2).[76] However, spectral complexity and interferences in the m/z 50–200 range make interpretation of small molecules more challenging. Once m/z values exceed 200, the O_2^- CIMS mass spectrum becomes clean, as shown in Fig. 2. This low-level mass spectral background is particularly advantageous for detecting high molecular weight compounds such as PFAS, and to the best of our knowledge, this capability has not previously been employed for this purpose, and all the previous O_2^- work only investigated compounds with m/z values <300.[69,70,72,77]

To understand the ionization chemistry of O_2^- as a regent ion, it is important to confirm the identities of the low m/z peaks when no analytes are present (Fig. 2) through high-resolution peak fitting and introducing perturbations of suspected reagent compounds to the system. When no analytes are present, the O_2^- CIMS mass spectrum has major peaks at m/z values of 32, 50, 60, 76 and 94 (Fig. 2). Peak fitting and CO_2 perturbations (Section S6) showed these correspond to O_2^-, $(H_2O)O_2^-$, CO_3^-, $(CO_2)O_2^-$, and $CO_2(H_2O)O_2^-$, respectively, which is consistent with previous studies.[72,76] These five peaks, which are produced from the primary reagent ion (O_2^-) readily interacting with H_2O and CO_2 in ambient air, will henceforth be called the five main reagent ions and used for normalization due to their fluctuations as analytes enter the IMR and react with them. Rationale for the selection of the reagent ion pool in O_2^- CIMS is described in Section S7. Other ion peaks (labeled in light blue) are not considered as part of the main reagent ions because either they are present in trace amounts, or they are a constant background most of the time and do not readily react with analytes.

Given that analyte signals are dependent on the availability of reagent ions at a given time, quantification requires normalization. In I^- CIMS, the sum of the signals of I^- and H_2OI^- are used as an approximate measure of the total reagent ion signal, which is then normalized per million counts as a normalization factor for all analyte signals, a standard data processing step.[62,66] This procedure accounts for both instrument variability and changing operating conditions. O_2^- CIMS has not previously been applied to PFAS measurements in air, there is no established uniform processing method. Whereas I^- CIMS analysis has established normalization, there is no such common practice for O_2^- CIMS. To address this, we normalized O_2^- CIMS analyte signals per million counts of the five main reagent ions described above to partially account for variations in humidity and CO_2 (eqn (1)). While this approach reduces variability associated with changing environmental

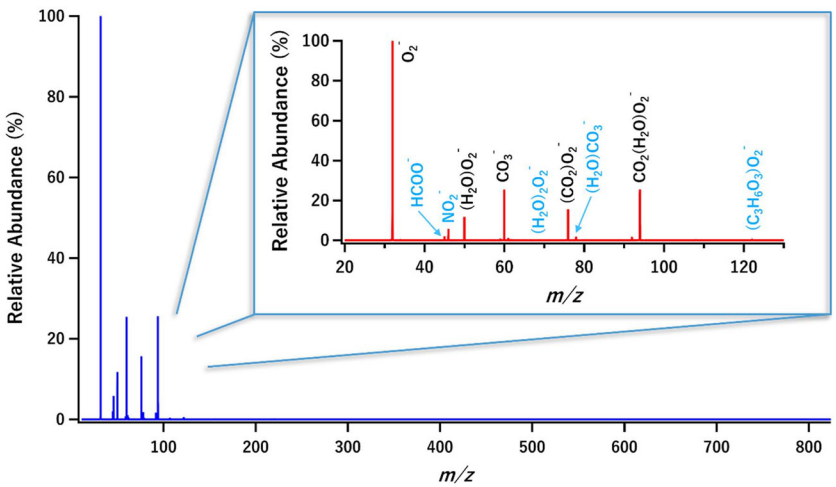

Fig. 2 General O_2^- CIMS mass spectrum with main reagent ions peaks (m/z 32, 50, 60, 76, and 94 corresponding to O_2^-, $(H_2O)O_2^-$, CO_3^-, $(CO_2)O_2^-$, $CO_2(H_2O)O_2^-$, respectively) labeled black and trace environmental ions labeled blue.

conditions, which is advantageous for indoor deployments where CO_2 levels fluctuate with ventilation and occupancy,[78] our results suggest that sensitivity variations associated with RH are not fully accounted for by this normalization, as discussed in Section S8.

$$\text{Normalized signal} = \frac{\text{analyte signal}}{\text{normalization factor}} = \frac{\text{analyte signal}}{\frac{\text{sum of } m/z\ 32,\ 50,\ 60,\ 76, \text{ and } 94}{10^6}}. \quad (1)$$

Solvent selection for calibration

Fig. 3 shows the main reagent ion fluctuations when a new solvent is introduced into the system. As PFAS calibration requires the selection of a suitable solvent, an ideal solvent must sufficiently dissolve the compound of interest, be volatile enough to carry standards to the CIMS for analysis, and have minimal impact on reagent ionization efficiency and distributions. We examined three candidate LC/MS grade solvents by injecting 20 μL of each (*i.e.*, methanol, acetonitrile, and ethyl acetate) without PFAS into the CIMS.

As shown in Fig. 3, although methanol consistently caused a decrease in the five main reagent ion peaks due to formation of the methanol-superoxide adduct at *m/z* 64, it produced the smallest change in the major reagent ion (O_2^-) and the decrease was uniform across all reagent ions. Acetonitrile caused larger, contrasting changes at *m/z* 32 (O_2^-) and 50 ($(H_2O)O_2^-$), while ethyl acetate resulted in the greatest fluctuations, most notably demonstrated by a nearly 25% decrease in O_2^-.

Based on these observations, methanol was selected as the solvent for blanks and PFAS standard preparation. This choice minimizes the impact on reagent ion distributions. Conveniently, most certified PFAS standards are supplied in methanol, simplifying laboratory preparation, and avoiding solvent incompatibility issues. While methanol yielded the most favorable results for calibration, acetonitrile remains a viable alternative, such as when standards are only available in acetonitrile or a PFAS has poor solubility in methanol.

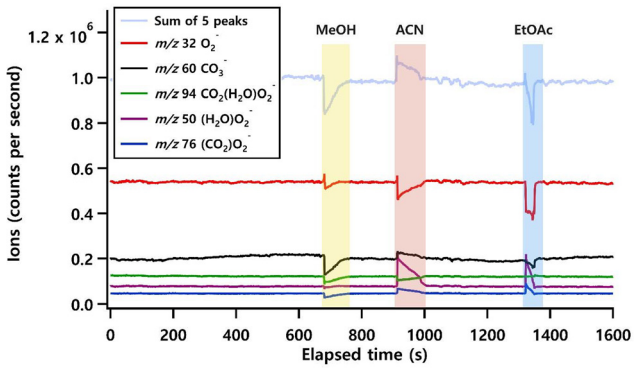

Fig. 3 O_2^- CIMS time series of main reagent ion peak response to methanol (MeOH, yellow shading), acetonitrile (ACN, red shading), and ethyl acetate (EtOAc, blue shading) in chronological order.

PFAS compounds detected

O_2^- CIMS appears to be sensitive to oxygenated semi-volatile PFAS compounds, including FTOHs, sulfonamides, epoxides, fluorotelomer diols (FTdiOH), and glycol ethers. However, some notable classes of PFAS were observed to have low sensitivity or no distinguishable signal, including perfluorinated carboxylic acids (PFCAs), fluorotelomer acrylates (FTACs), and perfluorinated sulfonic acids (PFSAs). It should be noted that PFCAs have been previously detected by I^- CIMS.[62,67,79] The 37 compounds tested for suitability with O_2^- CIMS and their detectability are summarized in Section S9 (Table S4).

While the multiple reagent ions of O_2^- CIMS can complicate mass spectra, they also offer distinct advantages. A common challenge in PFAS detection by CIMS is that FTOHs and PFCAs have similar masses (<0.05 Da), making it difficult for instruments with resolving power less than 10 000 to confidently distinguish and separate FTOHs in complex matrices based solely on mass.[64] As such, additional GC or LC separation is typically required for high-confidence confirmation of signal identification. O_2^- eliminates interference for FTOH measurements or otherwise enables deconvolution of I^- CIMS signals. With the potential to switch rapidly between I^- and O_2^- mode, it is possible to monitor both PFCAs and FTOHs. Moreover, O_2^- CIMS produces a characteristic series of peaks for $n:2$ FTOHs (n = 4, 6, 8, 10) at M + 46, M + 60, M + 78, M + 92, and M + 94 (Fig. S4), in addition to the main superoxide cluster (M + 32). These "fingerprint" ion peaks can aid in verifying the presence of FTOHs, much how tandem MS fragment ions are used in signal interpretation. For example, as shown in Fig. 4, the mass spectrum of a 6 : 2 FTOH standard closely matched that of a floor wax sample previously confirmed to contain 6 : 2 FTOH by GC/MS and I^- CIMS,[64] with identical fingerprint ion peaks observed. This finding suggests that, in some cases, ultra-high-resolution mass spectrometry or upstream GC/LC separation may not be necessary for compound identification when using O_2^- CIMS. While these fingerprint ion peaks are not used for quantitative purposes, they provide valuable complementary information for verification of PFAS compound identity as qualifying ions.

PFAS calibration results

All sensitivity calibration results are shown in Table 1, with comparisons to I^- CIMS addressed later (Table 2). Given the complexity of superoxide ionization, preliminary injections were performed to identify the major ion peaks used for calibration. Complete mass spectra of 14 individual PFAS compounds are provided in Section S10, along with detailed reasoning for calibration ion peaks selection in each figure caption. Calibrations were performed using methanol as the solvent at 50 ± 2% relative humidity (RH), where the humidity reflected ambient laboratory air (*i.e.*, room air measured at that level) and no additional humidification of the carrier gas was applied, which is representative of typical daytime outdoor

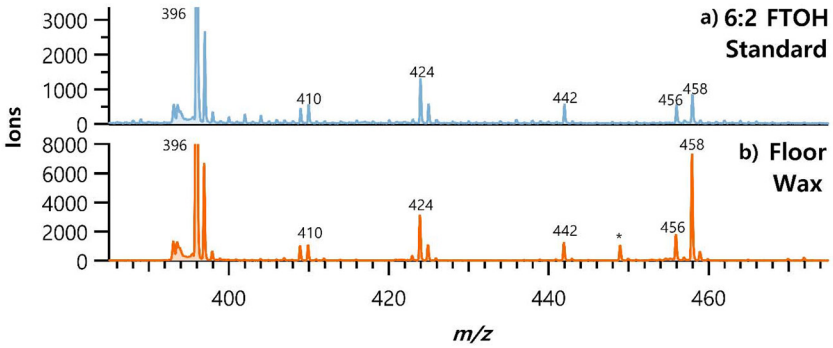

Fig. 4 Mass spectra obtained using O_2^- CIMS showing 6 : 2 FTOH fingerprint peaks comparison in (a) 1000 ng mL^{-1} 6 : 2 FTOH in methanol headspace sniff test, (b) brand name floor wax headspace sniff test. The *y*-axis was scaled to highlight the isotopic peak (*M* + 1 O_2^- adduct at *m*/*z* 397) and other diagnostic peaks. The peak marked with a star at *m*/*z* 449 originates from an unidentified background component in the floor wax. With increasing 6 : 2 FTOH concentration, a corresponding increase in the relative intensity of the *M* + 94 peak at *m*/*z* 458 was observed, and the 6 : 2 FTOH dimer with superoxide cluster was also detected (*m*/*z* 760). This trend was similarly observed for other *n* : 2 FTOHs. The mass error for *M* + 32 at *m*/*z* 396 ($C_8H_5F_{13}O_3^-$) is 14.6 parts per million (ppm), and for *M* + 94 at *m*/*z* 458 ($C_9H_7F_{13}O_6^-$) is 31 ppm.

Table 1 O_2^- CIMS calibration results

Compound	CAS #	Formula	Unit *m*/*z*	Calibrant ion peak (s) (*m*/*z*)	Sensitivity (ncps $pptv^{-1}$)	R^2	LOD (pptv)	LOQ (pptv)
4 : 2 FTOH	2043-47-2	$C_6H_5F_9O$	264	296	11.8 ± 0.3	0.9953	0.75	3.78
6 : 2 FTOH	647-42-7	$C_8H_5F_{13}O$	364	396	13.7 ± 0.4	0.9953	0.51	2.97
8 : 2 FTOH	678-39-7	$C_{10}H_5F_{17}O$	464	496	9.7 ± 0.2	0.9970	0.80	4.75
10 : 2 FTOH	865-86-1	$C_{12}H_5F_{21}O$	564	596	7.2 ± 0.2	0.9973	0.68	5.22
MeFOSA	31506-32-8	$C_9H_4F_{17}NO_2S$	513	512, 545	25.4 ± 0.5	0.9979	0.23	1.46
EtFOSA	4151-50-2	$C_{10}H_6F_{17}NO_2S$	527	526, 559	27.7 ± 0.4	0.9988	0.21	1.35
MeFOSE	24448-09-7	$C_{11}H_8F_{17}NO_3S$	557	589, 651	13.4 ± 0.4	0.9954	0.50	2.99
EtFOSE	1691-99-2	$C_{12}H_{10}F_{17}NO_3S$	571	603, 665	13.9 ± 0.5	0.9934	0.52	3.13
3-(Perfluorohexyl)propyl epoxide	38565-52-5	$C_9H_5F_{13}O$	376	408	0.124 ± 0.002	0.9992	68.61	362.53
3-(Perfluorooctyl)propyl epoxide	38565-53-6	$C_{11}H_5F_{17}O$	476	508	0.069 ± 0.001	0.9993	78.83	541.59
FBSA	30334-69-1	$C_4H_2F_9NO_2S$	299	298, 331, 359	48.3 ± 0.5	0.9993	0.38	1.55
1 : 8 : 1 FTdiOH	754-96-1	$C_{10}H_6F_{16}O_2$	462	461, 494, 556	21.3 ± 0.2	0.9995	0.64	3.06
Fluorinated triethylene glycol	129301-42-4	$C_6H_6F_8O_4$	294	293, 326. 388	22.9 ± 0.5	0.9975	0.12	1.38
Fluorinated tetraethylene glycol	330562-44-2	$C_8H_6F_{12}O_5$	410	307, 409, 442	41 ± 2	0.9920	0.07	0.72

conditions in the southeastern United States, despite expected seasonal and diurnal variability.[80,81] The sensitivities' dependency on the RH is discussed in Section S8 with FTOHs.

In some cases, more than one *m*/*z* value was used for quantification. In those cases, the normalized signals of selected ion peaks were summed and plotted against time, and the integrated areas were used to construct calibration curves. Calibration curves are provided in Section S11. The slope of each 8-point calibration curve represents the instrument's sensitivity, reported as normalized counts per second per parts per trillion by volume (ncps $pptv^{-1}$). R^2 values greater than 0.99 were calculated for the orthogonal linear regressions of all 14 calibrations. Furthermore, all calibrations yielded relative standard deviations below 10%, indicating acceptable precision for quantitative analysis. An example calibration plot of FTOHs, which have been quantified through many gas-phase methods,[62,67] is shown in Fig. 5.

When compared to I^- CIMS calibrations obtained using the CAMILS method by Davern *et al.*[62] (Table 2), O_2^- CIMS had higher sensitivity for five of the six compounds tested in both studies (*e.g.*, 270%, 220%, 160%, 126%, and 140% the sensitivity of 4 : 2 FTOH, 6 : 2 FTOH, 8 : 2 FTOH, 10 : 2 FTOH, and EtFOSA, respectively). The FTOHs all had lower LODs (*i.e.*, sub-pptv) using O_2^- CIMS, while the EtFOSA LOD was comparable.

Table 2 Comparison with Davern *et al.* I^- CIMS calibrations

Compound name/ abbreviation	Sensitivity (ncps $pptv^{-1}$)		LOD (pptv)	
	This study	Davern *et al.*[62]	This study	Davern *et al.*[62]
4 : 2 FTOH	11.8 ± 0.3	4.3 ± 0.01	0.75	3.1
6 : 2 FTOH	13.7 ± 0.4	6.1 ± 0.03	0.51	1.5
8 : 2 FTOH	9.7 ± 0.2	6.2 ± 0.06	0.8	2
10 : 2 FTOH	7.2 ± 0.2	5.7 ± 0.07	0.68	1.7
EtFOSA	27.7 ± 0.4	19.7[a]	0.21	0.2
1 : 8 : 1 FTdiOH	21.3 ± 0.2	46.9[a]	0.64	0.4
PFOA	ND	12.4 ± 0.2	NA	0.7
PFBA	ND	20.7 ± 0.3	NA	1.3
HFPO-DA	NA	23.1 ± 0.3	NA	0.7
E2	NA	0.0047	NA	1700

ND: not detected; NA: not applicable. [a] Standard deviations were not reported in Davern *et al.*

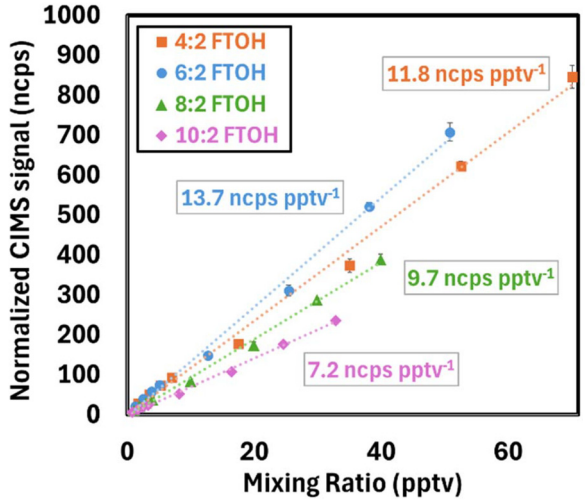

Fig. 5 FTOHs calibration plot, where 4 : 2 FTOH (orange and square), 6 : 2 FTOH (blue and round), 8 : 2 FTOH (green and triangle), 4 : 2 FTOH (purple and rhombus) is labeled in the figure. Best-fit orthogonal linear regressions are shown with dashed lines. Each calibration point was measured in triplicate on the same day, with error bars (black) representing the standard deviations of replicate measurements. All reported sensitivities are normalized per million counts of reagent ion signal.

However, O_2^- CIMS was 45% as sensitive to 1 : 8 : 1 FTdiOH, and it failed to significantly detect any of the PFCAs (*e.g.*, PFBA and PFOA) that Davern *et al.*[62] measured using I^- CIMS, suggesting that O_2^- reagent ion chemistry has a lower affinity for PFCAs. Furthermore, despite the similar instrument settings and the use of CAMILS, the uncertainties for the sensitivity in this study were greater than in Davern *et al.*,[62] likely due to the more complex and variable ionization pathways present in O_2^- reagent ion chemistry.

Real-time gas-phase FTOH emissions from fast-food packaging

When the food paper wrap was present, real-time 6 : 2 FTOH emissions from a consumer product at room temperature were detected. As shown in Fig. 6, even when the paper wrap was left undisturbed at 10 cm from the instrument inlet, the 6 : 2 FTOH concentration from food-paper wrap emissions was above the instrument's LOQ. Upon agitating the paper wrap by rubbing its surfaces together, higher 6 : 2 FTOH emissions were observed, with peak concentrations reaching up to 16 pptv. Once the paper wrap was removed from the vicinity of the inlet, the signal immediately returned to background levels, suggesting minimal measurement delays. This experiment highlights the potential for real-time PFAS air measurements and point-of-source determination using O_2^- CIMS, even for highly dynamic systems. Even though PFAS have previously been reported in food packaging and suggested to volatilize into indoor air,[10] the use of traditional offline methods required extensive sample collection, preparation, and extraction. The real-time (online) approach presented herein requires no sample preparation while providing highly time-resolved measurements. Supporting results, including GC/EI-MS verification for 6 : 2 FTOH and perturbation fingerprints of 6 : 2 FTOH, are provided in Section S12.

Limitations & further characterization

There are some limitations when using the O_2^- CIMS method. Although it offers safer reagent ion generation through elimination of the need for methyl iodide compared to I^- CIMS, it still relies on a commercially available sealed Po-210 radioactive source. Its use requires compliance with laboratory safety standards.[82] With a half-life of 138 days, the ion source must be replaced approximately once per year with notable decreases in absolute sensitivity happening before then. Another common challenge with general CIMS is the need for calibration prior to quantification, as well as the limited availability of standards for short-lived or otherwise highly reactive gas-phase analytes of interest. Thus, non-targeted PFAS analysis can be challenging,[83] but a GC separation upstream can help rule out complexities. Future work will examine the coupling of GC to CIMS for non-targeted PFAS detection.

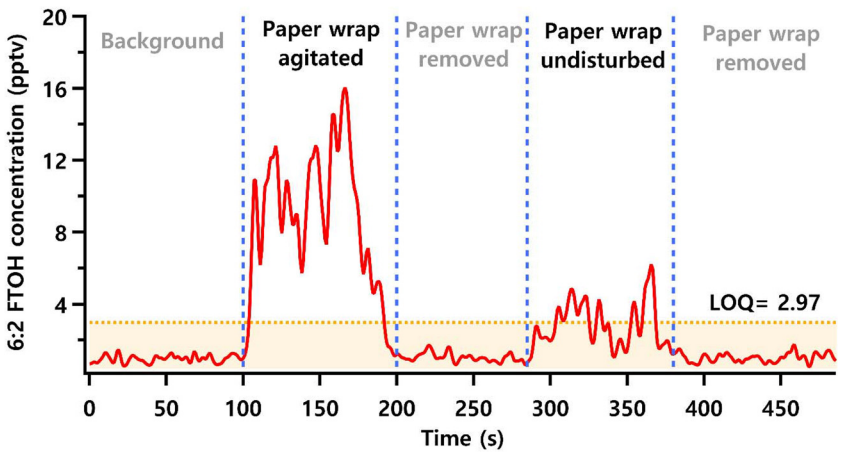

Fig. 6 Time series of 6 : 2 FTOH perturbation (shown in red) from a fast-food packaging paper wrap. The results are smoothed for 3 seconds to reduce fluctuations. Instrument LOQ of 2.97 pptv is shown with a yellow, dashed line calculated based on calibration results.

It is important to emphasize that the present work is intended as a feasibility study demonstrating the applicability of O_2^- CIMS to capture environmentally and industrially relevant classes of gas-phase PFAS like FTOHs, further analytical exploration is warranted. Due to the nature of this work being a feasibility study, future work should include systematic optimization of instrument voltages to balance declustering and analyte ion stability, incorporation of higher molecular weight calibration compounds to improve mass accuracy at high m/z, and further mechanistic characterization of ionization pathways alongside controlled studies of H_2O and CO_2 effects to establish a more rigorous normalization framework. Exploration of alternative ionization sources (*e.g.*, VUV lamps)[84] may also reduce radiation safety concerns and provide insight into differences in ionization behavior. In addition, expanding compound coverage and evaluating performance in complex matrices with coexisting VOCs will be important, potentially leveraging AI-assisted data analysis and spectral prediction.

Environmental implications and conclusions

The use of O_2^- as a reagent ion in CIMS demonstrates potential for real-time gas-phase measurement of PFAS in addition to other VOCs. Compared to I^- CIMS, O_2^- CIMS is safer and requires less ventilation, making it more suitable for field and mobile deployments, as well as space-constrained laboratory environments. It exhibits higher sensitivity and lower detection limits for FTOHs, making it well-suited for capturing transient gaseous FTOH emissions under ambient conditions. This capability highlights its potential for determining concentrations for a wide range of PFAS compounds relevant to occupational, residential, and ambient air environments. Real-time air measurements can also provide insight into PFAS sources and support the development of exposure mitigation strategies. Once calibrated, O_2^- CIMS can provide real-time quantitative PFAS measurements. For some PFAS compounds, distinct fingerprint ion peaks provide an additional dimension of confirmation, reducing reliance on offline separation methods such as GC-/LC-MS, thus saving time, cost, and analytical effort. Moreover, identical voltage and pressure settings shared between I^- and O_2^- CIMS parameters suggest the potential for rapid switching between these reagent ions, thereby facilitating deconvolution of CIMS signals and providing complementary dimensions of chemical information.

Author contributions

The manuscript was written through contributions of all authors. All authors have given approval to the final version of the manuscript. It is noted that Yufan Hu and Joji W. Sherman co-led this work in terms of the design and execution of the planned studies, and co-led the writing of this manuscript. As a result, they are co-first authors of this study.

Conflicts of interest

There are no conflicts to report.

Data availability

Raw and processed mass spectral data related to the method development, PFAS calibrations, and fast-food wrap will be deposited in the UNC Dataverse, a trustworthy, generalist data repository managed by the Research Data Management Core at the University of North Carolina at Chapel Hill. UNC Dataverse provides persistent identifiers, robust standardized metadata, and is committed to long-term preservation and access of research data. Data are published under a CC0 license by default with customizable terms of use as needed. Additionally, UNC Dataverse is routinely backed up and preserved on multiple geographically distributed servers and is a member of Data-PASS, a community committed to the sustainability and access of research data. Access to original data can be found at: https://doi.org/10.15139/S3/9SFZMS.

Supplementary information (SI): safety considerations, standards information and calibration preparation, a mass spectrum of 5 : 1 FTOH, permeation tube impacts on the reagent ions, O_2^- CIMS operating conditions and related parameters, confirmation of main reagent ion identities, rationale of reagent ions selection, sensitivities of FTOHs with different relative humidities (RH), a master list of calibration details, the mass spectra of all calibrated compounds along with discussions of the criteria used for selecting calibration ion peaks, calibration plots, and additional evidence of 6 : 2 FTOH detection in fast-food wraps. See DOI: https://doi.org/10.1039/d5an01352f.

Acknowledgements

This project was primarily supported by the North Carolina Collaboratory at The University of North Carolina at Chapel Hill with funding appropriated by the North Carolina General Assembly. This publication was also developed under Assistance Agreement No. R840431 awarded by the U. S. Environmental Protection Agency to University of North Carolina at Chapel Hill. It has not been formally reviewed by EPA. The views expressed in this document are solely those of authors and do not necessarily reflect those of the Agency. EPA does not endorse any products or commercial services mentioned in this publication. This work was also funded in part by the National Institute for Occupational Safety and Health (5T42OH008673).

References

1 K. Prevedouros, I. T. Cousins, R. C. Buck and S. H. Korzeniowski, Sources, Fate and Transport of Perfluorocarboxylates, *Environ. Sci. Technol.*, 2006, **40**, 32–44.

2 J. Glüge, M. Scheringer, I. T. Cousins, J. C. DeWitt, G. Goldenman, D. Herzke, R. Lohmann, C. A. Ng, X. Trier and Z. Wang, An overview of the uses of per- and polyfluoroalkyl substances (PFAS), *Environ. Sci. Process. Impacts*, 2020, **22**, 2345–2373.
3 L. G. T. Gaines, Historical and current usage of per- and polyfluoroalkyl substances (PFAS): A literature review, *Am. J. Ind. Med.*, 2023, **66**, 353–378.
4 Z. Wang, J. C. DeWitt, C. P. Higgins and I. T. Cousins, A Never-Ending Story of Per- and Polyfluoroalkyl Substances (PFASs)?, *Environ. Sci. Technol.*, 2017, **51**, 2508–2518.
5 I. van der Veen, S. Schellenberger, A.-C. Hanning, A. Stare, J. de Boer, J. M. Weiss and P. E. G. Leonards, Fate of Per- and Polyfluoroalkyl Substances from Durable Water-Repellent Clothing during Use, *Environ. Sci. Technol.*, 2022, **56**, 5886–5897.
6 G. Glenn, R. Shogren, X. Jin, W. Orts, W. Hart-Cooper and L. Olson, Per- and polyfluoroalkyl substances and their alternatives in paper food packaging, *Compr. Rev. Food Sci. Food Saf.*, 2021, **20**, 2596–2625.
7 L. A. Schaider, S. A. Balan, A. Blum, D. Q. Andrews, M. J. Strynar, M. E. Dickinson, D. M. Lunderberg, J. R. Lang and G. F. Peaslee, Fluorinated Compounds in U. S. Fast Food Packaging, *Environ. Sci. Technol. Lett.*, 2017, **4**, 105–111.
8 M. Sajid and M. Ilyas, PTFE-coated non-stick cookware and toxicity concerns: a perspective, *Environ. Sci. Pollut. Res.*, 2017, **24**, 23436–23440.
9 G. Guerrero-Vacas, F. Comino and O. Rodríguez-Alabanda, Evaluation of the effectiveness and durability of commercial non-stick coatings, *J. Food Eng.*, 2024, **370**, 111959.
10 H. Schwartz-Narbonne, C. Xia, A. Shalin, H. D. Whitehead, D. Yang, G. F. Peaslee, Z. Wang, Y. Wu, H. Peng, A. Blum, M. Venier and M. L. Diamond, Per- and Polyfluoroalkyl Substances in Canadian Fast Food Packaging, *Environ. Sci. Technol. Lett.*, 2023, **10**, 343–349.
11 J. Glüge, K. Breuer, A. Hafner, C. Vering, D. Müller, I. T. Cousins, R. Lohmann, G. Goldenman and M. Scheringer, Finding non-fluorinated alternatives to fluorinated gases used as refrigerants, DOI: 10.1039/D4EM00444B.
12 D. J. Seow, Fire Fighting Foams with Perfluorochemicals-Environmental Review.
13 K. Pozo, L. B. Moreira, P. Karaskova, P. Přibylová, J. Klánová, M. U. de Carvalho, L. A. Maranho, D. M and A. de Souza, Using large amounts of firefighting foams releases per- and polyfluoroalkyl substances (PFAS) into estuarine environments: A baseline study in Latin America, *Mar. Pollut. Bull.*, 2022, **182**, 113938.
14 G. F. Peaslee, J. T. Wilkinson, S. R. McGuinness, M. Tighe, N. Caterisano, S. Lee, A. Gonzales, M. Roddy, S. Mills and K. Mitchell, Another Pathway for Firefighter Exposure to Per- and Polyfluoroalkyl Substances: Firefighter Textiles, *Environ. Sci. Technol. Lett.*, 2020, **7**, 594–599.
15 I. T. Cousins, J. C. DeWitt, J. Glüge, G. Goldenman, D. Herzke, R. Lohmann, M. Miller, C. A. Ng, M. Scheringer, L. Vierke and Z. Wang, Strategies for grouping per- and polyfluoroalkyl substances (PFAS) to protect human and environmental health, DOI: 10.1039/D0EM00147C.
16 M. G. Evich, M. J. B. Davis, J. P. McCord, B. Acrey, J. A. Awkerman, D. R. U. Knappe, A. B. Lindstrom, T. F. Speth, C. Tebes-Stevens, M. J. Strynar, Z. Wang, E. J. Weber, W. M. Henderson and J. W. Washington, Per- and polyfluoroalkyl substances in the environment, *Science*, 2022, **375**, eabg9065.
17 L. Zhao, L. Zhu, S. Zhao and X. Ma, Sequestration and bioavailability of perfluoroalkyl acids (PFAAs) in soils: Implications for their underestimated risk, *Sci. Total Environ.*, 2016, **572**, 169–176.
18 J. P. Giesy and K. Kannan, Global Distribution of Perfluorooctane Sulfonate in Wildlife, *Environ. Sci. Technol.*, 2001, **35**, 1339–1342.
19 P. Zareitalabad, J. Siemens, M. Hamer and W. Amelung, Perfluorooctanoic acid (PFOA) and perfluorooctanesulfonic acid (PFOS) in surface waters, sediments, soils and wastewater – A review on concentrations and distribution coefficients, *Chemosphere*, 2013, **91**, 725–732.
20 A. O. De Silva, C. Spencer, B. F. Scott, S. Backus and D. C. G. Muir, Detection of a Cyclic Perfluorinated Acid, Perfluoroethylcyclohexane Sulfonate, in the Great Lakes of North America, *Environ. Sci. Technol.*, 2011, **45**, 8060–8066.
21 K. Y. Christensen, M. Raymond, M. Blackowicz, Y. Liu, B. A. Thompson, H. A. Anderson and M. Turyk, Perfluoroalkyl substances and fish consumption, *Environ. Res.*, 2017, **154**, 145–151.
22 P. Grandjean, E. W. Andersen, E. Budtz-Jørgensen, F. Nielsen, K. Mølbak, P. Weihe and C. Heilmann, Serum Vaccine Antibody Concentrations in Children Exposed to Perfluorinated Compounds, *J. Am. Med. Assoc.*, 2012, **307**, 391–397.
23 E. M. Sunderland, X. C. Hu, C. Dassuncao, A. K. Tokranov, C. C. Wagner and J. G. Allen, A review of the pathways of human exposure to poly- and perfluoroalkyl substances (PFASs) and present understanding of health effects, *J. Expo. Sci. Environ. Epidemiol.*, 2019, **29**, 131–147.
24 V. M. Vieira, K. Hoffman, H.-M. Shin, J. M. Weinberg, T. F. Webster and T. Fletcher, Perfluorooctanoic Acid Exposure and Cancer Outcomes in a Contaminated Community: A Geographic Analysis, *Environ. Health Perspect.*, 2013, **121**, 318–323.
25 N. Johansson, A. Fredriksson and P. Eriksson, Neonatal exposure to perfluorooctane sulfonate (PFOS) and perfluorooctanoic acid (PFOA) causes neurobehavioural defects in adult mice, *NeuroToxicology*, 2008, **29**, 160–169.
26 T. G. Ambaye, M. Vaccari, S. Prasad and S. Rtimi, Recent progress and challenges on the removal of per- and polyfluoroalkyl substances (PFAS) from contaminated soil and water, *Environ. Sci. Pollut. Res.*, 2022, **29**, 58405–58428.
27 K. H. Kucharzyk, R. Darlington, M. Benotti, R. Deeb and E. Hawley, Novel treatment technologies for PFAS compounds: A critical review, *J. Environ. Manage.*, 2017, **204**, 757–764.

28 B. C. Crone, T. F. Speth, D. G. Wahman, S. J. Smith, G. Abulikemu, E. J. Kleiner and J. G. Pressman, Occurrence of per- and polyfluoroalkyl substances (PFAS) in source water and their treatment in drinking water, *Crit. Rev. Environ. Sci. Technol.*, 2019, **49**, 2359–2396.

29 E. Kumarasamy, I. M. Manning, L. B. Collins, O. Coronell and F. A. Leibfarth, Ionic Fluorogels for Remediation of Per- and Polyfluorinated Alkyl Substances from Water, *ACS Cent. Sci.*, 2020, **6**, 487–492.

30 I. M. Manning, N. Guan Pin Chew, H. P. Macdonald, K. E. Miller, M. J. Strynar, O. Coronell and F. A. Leibfarth, Hydrolytically Stable Ionic Fluorogels for High-Performance Remediation of Per- and Polyfluoroalkyl Substances (PFAS) from Natural Water, *Angew. Chem.*, 2022, **134**, e202208150.

31 K. Weitz, D. Kantner, A. Kessler, H. Key, J. Larson, W. Bodnar, S. Parvathikar, L. Davis, N. Robey, P. Taylor, F. De la Cruz, T. Tolaymat, N. Weber, W. Linak, J. Krug and L. Phelps, Review of per- and poly-fluoroalkyl treatment in combustion-based thermal waste systems in the United States, *Sci. Total Environ.*, 2024, **932**, 172658.

32 G. R. Johnson, PFAS in soil and groundwater following historical land application of biosolids, *Water Res.*, 2022, **211**, 118035.

33 Y. Hu, H. Chen, Y. Chen, Y. Wang, Y. Luo, L. Sang, T. Jin and S. Wu, Perfluoroalkyl acids (PFAAs) and their precursors in sediments and adjacent riparian soils from the Three Gorges Reservoir, China: Contamination characteristics, source apportionment and ecological risks, *Environ. Res.*, 2025, **274**, 121202.

34 O. US EPA, Per- and Polyfluoroalkyl Substances (PFAS), https://www.epa.gov/sdwa/and-polyfluoroalkyl-substances-pfas, (accessed 23 August 2025).

35 T. Teymoorian, G. Munoz, S. Vo Duy, J. Liu and S. Sauvé, Tracking PFAS in Drinking Water: A Review of Analytical Methods and Worldwide Occurrence Trends in Tap Water and Bottled Water, *ACS ES&T Water*, 2023, **3**, 246–261.

36 S. J. Chow, N. Ojeda, J. G. Jacangelo and K. J. Schwab, Detection of ultrashort-chain and other per- and polyfluoroalkyl substances (PFAS) in U.S. bottled water, *Water Res.*, 2021, **201**, 117292.

37 C. Gremmel, T. Frömel and T. P. Knepper, HPLC–MS/MS methods for the determination of 52 perfluoroalkyl and polyfluoroalkyl substances in aqueous samples, *Anal. Bioanal. Chem.*, 2017, **409**, 1643–1655.

38 X. Li, W. Li, Z. Wang, X. Wang, Y. Cai and Y. Shi, Atmospheric Emission of Per- and Polyfluoroalkyl Substances (PFAS) from a Fluoropolymer Manufacturing Facility: Focus on Emerging PFAS and the Potential Contribution of Condensable PFAS on their Atmospheric Partitioning, *Environ. Sci. Technol.*, 2025, **59**, 9709–9720.

39 W.-L. Li and K. Kannan, Determination of Legacy and Emerging Per- and Polyfluoroalkyl Substances (PFAS) in Indoor and Outdoor Air, *ACS ES&T Air*, 2024, **1**, 1147–1155.

40 D. Persaud, A. S. Criscitiello, C. Spencer, I. Lehnherr, D. C. G. Muir, A. O. D. Silva and C. J. Young, A 50 years record for perfluoroalkyl acids in the high arctic: implications for global and local transport, *Environ. Sci. Process. Impacts*, 2024, **26**, 1543–1555.

41 J. J. MacInnis, K. French, D. C. G. Muir, C. Spencer, A. Criscitiello, A. O. D. Silva and C. J. Young, Emerging investigator series: a 14-year depositional ice record of perfluoroalkyl substances in the High Arctic, *Environ. Sci. Process. Impacts*, 2017, **19**, 22–30.

42 F. Wania, A Global Mass Balance Analysis of the Source of Perfluorocarboxylic Acids in the Arctic Ocean, *Environ. Sci. Technol.*, 2007, **41**, 4529–4535.

43 R. Holland, M. A. H. Khan, R. Chhantyal-Pun, A. J. Orr-Ewing, C. J. Percival, C. A. Taatjes and D. E. Shallcross, Investigating the Atmospheric Sources and Sinks of Perfluorooctanoic Acid Using a Global Chemistry Transport Model, *Atmosphere*, 2020, **11**, 407.

44 E. L. D'Ambro, H. O. T. Pye, J. O. Bash, J. Bowyer, C. Allen, C. Efstathiou, R. C. Gilliam, L. Reynolds, K. Talgo and B. N. Murphy, Characterizing the Air Emissions, Transport, and Deposition of Per- and Polyfluoroalkyl Substances from a Fluoropolymer Manufacturing Facility, *Environ. Sci. Technol.*, 2021, **55**, 862–870.

45 J. Garnett, C. Halsall, H. Winton, H. Joerss, R. Mulvaney, R. Ebinghaus, M. Frey, A. Jones, A. Leeson and P. Wynn, Increasing Accumulation of Perfluorocarboxylate Contaminants Revealed in an Antarctic Firn Core (1958–2017), *Environ. Sci. Technol.*, 2022, **56**, 11246–11255.

46 J. Roostaei, S. Colley, R. Mulhern, A. A. May and J. M. Gibson, Predicting the risk of GenX contamination in private well water using a machine-learned Bayesian network model, *J. Hazard. Mater.*, 2021, **411**, 125075.

47 J. E. Galloway, A. V. P. Moreno, A. B. Lindstrom, M. J. Strynar, S. Newton, A. A. May and L. K. Weavers, Evidence of Air Dispersion: HFPO–DA and PFOA in Ohio and West Virginia Surface Water and Soil near a Fluoropolymer Production Facility, *Environ. Sci. Technol.*, 2020, **54**, 7175–7184.

48 R. Wu, H. Lin, E. Yamazaki, S. Taniyasu, M. Sörengård, L. Ahrens, P. K. S. Lam, H. Eun and N. Yamashita, Simultaneous analysis of neutral and ionizable per- and polyfluoroalkyl substances in air, *Chemosphere*, 2021, **280**, 130607.

49 H. P. H. Arp and K.-U. Goss, Irreversible sorption of trace concentrations of perfluorocarboxylic acids to fiber filters used for air sampling, *Atmos. Environ.*, 2008, **42**, 6869–6872.

50 J. L. Barber, U. Berger, C. Chaemfa, S. Huber, A. Jahnke, C. Temme and K. C. Jones, Analysis of per- and polyfluorinated alkyl substances in air samples from Northwest Europe, *J. Environ. Monit.*, 2007, **9**, 530–541.

51 N. Y. Chang, C. M. A. Eichler, D. E. Amparo, J. Zhou, K. Baumann, E. A. C. Hubal, J. D. Surratt, G. C. Morrison and B. J. Turpin, Indoor air concentrations of PM2.5 quartz fiber filter-collected ionic PFAS and emissions to outdoor air: findings from the IPA campaign, *Environ. Sci. Process. Impacts*, 2025, **27**, 1603–1618.

52 S. Mok, S. Lee, Y. Choi, J. Jeon, Y. H. Kim and H.-B. Moon, Target and non-target analyses of neutral per- and polyfluoroalkyl substances from fluorochemical industries using GC-MS/MS and GC-TOF: Insights on their environmental fate, *Environ. Int.*, 2023, **182**, 108311.

53 W. Zhang, L. Xu and H. Zhang, Recent advances in mass spectrometry techniques for atmospheric chemistry research on molecular-level, *Mass Spectrom. Rev.*, 2024, **43**, 1091–1134.

54 L. G. Huey, Measurement of trace atmospheric species by chemical ionization mass spectrometry: Speciation of reactive nitrogen and future directions, *Mass Spectrom. Rev.*, 2007, **26**, 166–184.

55 T. H. Bertram, J. R. Kimmel, T. A. Crisp, O. S. Ryder, R. L. N. Yatavelli, J. A. Thornton, M. J. Cubison, M. Gonin and D. R. Worsnop, A field-deployable, chemical ionization time-of-flight mass spectrometer, *Atmos. Meas. Tech.*, 2011, **4**, 1471–1479.

56 Vocus - Aerodyne, https://aerodyne.com/gas-phase-analyzers/vocus/, (accessed 17 February 2025).

57 A. R. Koss, C. Warneke, B. Yuan, M. M. Coggon, P. R. Veres and J. A. de Gouw, Evaluation of NO^+ reagent ion chemistry for online measurements of atmospheric volatile organic compounds, *Atmos. Meas. Tech.*, 2016, **9**, 2909–2925.

58 B. Yuan, A. Koss, C. Warneke, J. B. Gilman, B. M. Lerner, H. Stark and J. A. de Gouw, A high-resolution time-of-flight chemical ionization mass spectrometer utilizing hydronium ions (H_3O^+ ToF-CIMS) for measurements of volatile organic compounds in the atmosphere, *Atmos. Meas. Tech.*, 2016, **9**, 2735–2752.

59 S. Gagan, M. Olin, A. J. Dodero, S. Gopalakrishnan, S. Niu, M. J. Davern, B. J. Turpin, J. D. Surratt and Y. Zhang, Real-Time Identification and Quantification of Per- and Polyfluoroalkyl Substances Using High-Resolution Time-of-Flight Chemical Ionization Mass Spectrometry with Positive Reagent Ions, *Anal. Chem.*, 2026, **98**, 124–133.

60 M. Riva, P. Rantala, J. E. Krechmer, O. Peräkylä, Y. Zhang, L. Heikkinen, O. Garmash, C. Yan, M. Kulmala, D. Worsnop and M. Ehn, Evaluating the performance of five different chemical ionization techniques for detecting gaseous oxygenated organic species, *Atmos. Meas. Tech.*, 2019, **12**, 2403–2421.

61 J. M. Mattila, J. D. Krug, W. R. Roberson, R. P. Burnette, S. McDonald, L. Virtaranta, J. H. Offenberg and W. P. Linak, Characterizing Volatile Emissions and Combustion Byproducts from Aqueous Film-Forming Foams Using Online Chemical Ionization Mass Spectrometry, *Environ. Sci. Technol.*, 2024, **58**, 3942–3952.

62 M. J. Davern, G. V. West, C. M. A. Eichler, B. J. Turpin, Y. Zhang and J. D. Surratt, External liquid calibration method for iodide chemical ionization mass spectrometry enables quantification of gas-phase per- and polyfluoroalkyl substances (PFAS) dynamics in indoor air, *Analyst*, 2024, **149**, 3405–3415.

63 J. Zhou, K. Baumann, N. Chang, G. Morrison, W. Bodnar, Z. Zhang, J. M. Atkin, J. D. Surratt and B. J. Turpin, Per- and polyfluoroalkyl substances (PFASs) in airborne particulate matter (PM2.0) emitted during floor waxing: A pilot study, *Atmos. Environ.*, 2022, **268**, 118845.

64 M. J. Davern, Y. Hu, G. V. West, Y. Kim, M. H. Francini, G. C. Morrison, Y. Zhang, B. J. Turpin and J. D. Surratt, Online Iodide Chemical Ionization Mass Spectrometry (I-CIMS) Enables Occupational Inhalation Exposure Assessment of 6 : 2 Fluorotelomer Alcohol (6 : 2 FTOH) Emitted to Air during Floor Waxing, *Environ. Sci. Technol. Lett.*, 2025, **12**, 607–612.

65 C. M. A. Eichler, M. J. Davern, J. D. Surratt, G. C. Morrison and B. J. Turpin, Fluorotelomer alcohol (FTOH) emission rates from new and old rain jackets to air determined by iodide high-resolution chemical ionization mass spectrometry, *Indoor Environ.*, 2024, **1**, 100055.

66 T. H. Bertram, J. R. Kimmel, T. A. Crisp, O. S. Ryder, R. L. N. Yatavelli, J. A. Thornton, M. J. Cubison, M. Gonin and D. R. Worsnop, A field-deployable, chemical ionization time-of-flight mass spectrometer, *Atmos. Meas. Tech.*, 2011, **4**, 1471–1479.

67 T. P. Riedel, J. R. Lang, M. J. Strynar, A. B. Lindstrom and J. H. Offenberg, Gas-Phase Detection of Fluorotelomer Alcohols and Other Oxygenated Per- and Polyfluoroalkyl Substances by Chemical Ionization Mass Spectrometry, *Environ. Sci. Technol. Lett.*, 2019, **6**, 289–293.

68 C. Ye, B. Yuan, Y. Lin, Z. Wang, W. Hu, T. Li, W. Chen, C. Wu, C. Wang, S. Huang, J. Qi, B. Wang, C. Wang, W. Song, X. Wang, E. Zheng, J. E. Krechmer, P. Ye, Z. Zhang, X. Wang, D. R. Worsnop and M. Shao, Chemical characterization of oxygenated organic compounds in the gas phase and particle phase using iodide CIMS with FIGAERO in urban air, *Atmos. Chem. Phys.*, 2021, **21**, 8455–8478.

69 X. Li, Y. Li, M. J. Lawler, J. Hao, J. N. Smith and J. Jiang, Composition of Ultrafine Particles in Urban Beijing: Measurement Using a Thermal Desorption Chemical Ionization Mass Spectrometer, *Environ. Sci. Technol.*, 2021, **55**, 2859–2868.

70 G. A. Novak, M. P. Vermeuel and T. H. Bertram, Simultaneous detection of ozone and nitrogen dioxide by oxygen anion chemical ionization mass spectrometry: a fast-time-response sensor suitable for eddy covariance measurements, *Atmos. Meas. Tech.*, 2020, **13**, 1887–1907.

71 M. P. Vermeuel, G. A. Novak, H. D. Alwe, D. D. Hughes, R. Kaleel, A. F. Dickens, D. Kenski, A. C. Czarnetzki, E. A. Stone, C. O. Stanier, R. B. Pierce, D. B. Millet and T. H. Bertram, Sensitivity of Ozone Production to NOx and VOC Along the Lake Michigan Coastline, *J. Geophys. Res.: Atmos.*, 2019, **124**, 10989–11006.

72 D. W. O'Sullivan, I. K. C. Silwal, A. S. McNeill, V. Treadaway and B. G. Heikes, Quantification of gas phase hydrogen peroxide and methyl peroxide in ambient air: Using atmospheric pressure chemical ionization mass spectrometry with O2−, and O2−(CO2) reagent ions, *Int. J. Mass Spectrom.*, 2018, **424**, 16–26.

73 F. Heydebreck, J. Tang, Z. Xie and R. Ebinghaus, Emissions of Per- and Polyfluoroalkyl Substances in a Textile

Manufacturing Plant in China and Their Relevance for Workers' Exposure, *Environ. Sci. Technol.*, 2016, **50**, 10386–10396.

74 J. N. Rewerts, J. T. Morré, S. L. Massey Simonich and J. A. Field, In-Vial Extraction Large Volume Gas Chromatography Mass Spectrometry for Analysis of Volatile PFASs on Papers and Textiles, *Environ. Sci. Technol.*, 2018, **52**, 10609–10616.

75 B. H. Lee, F. D. Lopez-Hilfiker, C. Mohr, T. Kurtén, D. R. Worsnop and J. A. Thornton, An Iodide-Adduct High-Resolution Time-of-Flight Chemical-Ionization Mass Spectrometer: Application to Atmospheric Inorganic and Organic Compounds, *Environ. Sci. Technol.*, 2014, **48**, 6309–6317.

76 G. A. Novak, M. P. Vermeuel and T. H. Bertram, Simultaneous detection of ozone and nitrogen dioxide by oxygen anion chemical ionization mass spectrometry: a fast-time-response sensor suitable for eddy covariance measurements, *Atmos. Meas. Tech.*, 2020, **13**, 1887–1907.

77 L. C. Chen, Z. Yu and K. Hiraoka, Vapor phase detection of hydrogen peroxide with ambient sampling chemi/chemical ionization mass spectrometry, *Anal. Methods*, 2010, **2**, 897–900.

78 D. Bastien, D. Licina, L. Bourikas, S. Crosby, S. Gauthier, I. Mino-Rodriguez and C. Piselli, The impact of real-time carbon dioxide awareness on occupant behavior and ventilation rates in student dwellings, *Energy Build.*, 2024, **310**, 114132.

79 C. J. Young, S. Joudan, Y. Tao, J. J. B. Wentzell and J. Liggio, High Time Resolution Ambient Observations of Gas-Phase Perfluoroalkyl Carboxylic Acids: Implications for Atmospheric Sources, *Environ. Sci. Technol. Lett.*, 2024, **11**, 1348–1354.

80 D. J. Gaffen and R. J. Ross, Climatology and Trends of U.S. Surface Humidity and Temperature.

81 L. Jia, T. L. Delworth, X. Yang, W. Cooke, N. C. Johnson, L. Zhang, Y. Joh, F. Lu and C. McHugh, Seasonal predictions of summer compound humid heat extremes in the southeastern United States driven by sea surface temperatures, *npj Clim. Atmos. Sci.*, 2024, **7**, 180.

82 Y. R. Lee, Y. Ji, D. J. Tanner and L. G. Huey, A low-activity ion source for measurement of atmospheric gases by chemical ionization mass spectrometry, *Atmos. Meas. Tech.*, 2020, **13**, 2473–2480.

83 M. Heinritzi, M. Simon, G. Steiner, A. C. Wagner, A. Kürten, A. Hansel and J. Curtius, Characterization of the mass-dependent transmission efficiency of a CIMS, *Atmos. Meas. Tech.*, 2016, **9**, 1449–1460.

84 Y. Ji, L. G. Huey, D. J. Tanner, Y. R. Lee, P. R. Veres, J. A. Neuman, Y. Wang and X. Wang, A vacuum ultraviolet ion source (VUV-IS) for iodide–chemical ionization mass spectrometry: a substitute for radioactive ion sources, *Atmos. Meas. Tech.*, 2020, **13**, 3683–3696.